

Evaluation of the impact of surfactants on miscibility of griseofulvin in spray dried amorphous solid dispersions

Article

Accepted Version

Bhanderi, A., Bari, F. and Al-Obaidi, H. ORCID:
<https://orcid.org/0000-0001-9735-0303> (2021) Evaluation of the impact of surfactants on miscibility of griseofulvin in spray dried amorphous solid dispersions. *Journal of Drug Delivery Science and Technology*, 64. 102606. ISSN 1773-2247 doi: 10.1016/j.jddst.2021.102606 Available at <https://centaur.reading.ac.uk/98743/>

It is advisable to refer to the publisher's version if you intend to cite from the work. See [Guidance on citing](#).

To link to this article DOI: <http://dx.doi.org/10.1016/j.jddst.2021.102606>

Publisher: Elsevier

All outputs in CentAUR are protected by Intellectual Property Rights law, including copyright law. Copyright and IPR is retained by the creators or other copyright holders. Terms and conditions for use of this material are defined in the [End User Agreement](#).

www.reading.ac.uk/centaur

CentAUR

Central Archive at the University of Reading

Reading's research outputs online

Evaluation of the impact of surfactants on miscibility of griseofulvin in spray dried amorphous solid dispersions

Amit Bhandari, Fiza Bari, Hisham Al-Obaidi*

The School of Pharmacy, University of Reading, Reading RG6 6AD, UK

The School of Pharmacy

University of Reading

Whiteknights, PO Box 226

RG6 6AP

Reading, UK

T: +44 118 378 6261

h.al-obaidi@reading.ac.uk

Keywords: Amorphous solid dispersions, surfactants, miscibility, solubility, glass transition temperature, Flory-Huggins

41 **Abstract**

42 The aim of this contribution is to examine the impact of incorporating surfactants into
43 amorphous solid dispersions on solid state miscibility and aqueous solubility of the antifungal
44 drug griseofulvin. Spray dried amorphous solid dispersions of griseofulvin (GF) and
45 hypromellose acetate succinate (HPMCAS) were prepared by spray drying. Three different
46 surfactants of varying ratios between 1 to 5% were used namely the anionic sodium dodecyl
47 sulfate (SDS), the cationic dodecyletrimethylammonium bromide (DTAB) and the non-ionic
48 pluronic (F127). Flory-Huggins model combined with calculations based on Hoffman's equation
49 were used to calculate miscibility and predicted solubility of the amorphous form. The results
50 showed that the prepared solid dispersions exhibited enhanced drug-polymer miscibility
51 reflected by improved thermodynamics of mixing. The highest miscibility was achieved when
52 DTAB was incorporated by which the drug-polymer miscibility was enhanced by approximately
53 1.5 times. The tendency to recrystallize was calculated using reduced recrystallization
54 parameter and correlated with the measured saturation solubility showing distinct properties
55 which were dependent on the type of surfactant. Saturated solubility of the solid dispersions
56 was compared with micellar solubility and was found to be significantly affected by the presence
57 of the polymer. The glass transition temperature (T_g) decreased significantly upon the addition
58 of surfactants. However, gravimetric analysis showed that solvent content did not exceed 1%
59 which suggests that the shifted T_g was not related to plasticizing effect of residual solvent.
60 Overall, these results suggest potential role for the surfactants in enhancing solid state
61 miscibility when incorporated into the solid dispersions.

64 **Introduction**

65 Converting crystalline drugs to the amorphous form has been accepted as effective approach to
66 improve solubility of hydrophobic drugs [1-3]. The favourable amorphous form has a higher
67 energy manifesting in higher apparent solubility and enhanced dissolution rates compared to
68 the crystalline form of the drug [4, 5]. Formation of amorphous solid dispersions has been
69 commonly used to formulate amorphous drugs. However, the amorphous form is
70 thermodynamically unstable and tend to re-crystallize over a period of time [6]. Recrystallization
71 can occur during storage (solid-state-mediated) or after administration of the drug (solution-
72 mediated), or both. Use of solid dispersions in which the drug is molecularly mixed with a
73 hydrophilic polymer has been successful in preventing recrystallization of the amorphous drug
74 [7].

One potential event that can be difficult to predict is whether the drug would remain amorphous upon exposure to the aqueous medium. This is particularly difficult to measure for fragile glass formers because of their high tendency to recrystallize [8]. We have shown before that a memory exists in solid particles where properties (such as formed H-bonds) in the solid state remained even after the drug has completely dissolved [9]. Hence it is possible to maintain drug-polymer interactions so that to improve the solubility of the poorly soluble drug. The latter can be achieved via enhancing drug-polymer solid state miscibility. Apart from amorphous form formation, incorporation of surfactants in the solid dispersion can be used as additional method to improve solubility. Previous studies have shown that anionic surfactants had a significant effect on the binding of GF to the polymer polyethylene glycol [10]. This was attributed to counterions forming a bridge between the polymer causing the aggregation of anionic surfactant and GF. This effect will not be seen with a non-ionic surfactant and will be smaller for cationic surfactants. The impact of the counterion on the properties of the dispersion has been studied and was shown to vary according to the charge to radius ratio [11]. For example, compared to K^+ and Na^+ , Li^+ has a larger charge/radius causing it to exhibit greater binding ability between the polymer and the drug; therefore Li^+ counterions have greater impact on the properties of the dispersion [11].

In a more recent study, the anionic surfactant sodium dodecyl sulfate (SDS) was shown to enhance nucleation of hesperetin crystals but equally slowing down crystal growth [12]. There are other studies in the literature which have investigated the impact of surfactants on the interactions of drug and polymer in solid dispersions. For example, impact of crystallization of itraconazole was studied in solid dispersions that included sodium lauryl sulfate and d- α -tocopheryl polyethylene glycol 1000 succinate. The authors showed that sodium lauryl sulfate/Soluplus[®] improved solid state stability and solubility of itraconazole [13]. In a different study, surfactants were found to interfere with the crystallization inhibitory efficiency of the polymers in spray dried amorphous solid dispersions [13].

Despite previous research, we believe that the impact of surfactants on induction/inhibition of recrystallization of amorphous drugs is still not well understood. This stems from our previous work in which we have shown that surfactants displayed different behaviour in terms of their impact on drug polymer miscibility depending on the method of preparation [14]. Here in this work, we use thermal analysis to measure the impact of surfactants on solid state miscibility of the drug and the polymer. This approach is based on measuring configurational energy of the amorphous form and calculate solubility ratio (amorphous/crystalline). We compare the results

with predictions made using Flory-Huggins model based on analysing physical mixtures of the drug/polymer/surfactant. The prepared amorphous solid dispersions contain griseofulvin (GF) as the model drug which is known to exhibit low aqueous solubility while the polymer is hypromellose acetate succinate (HPMCAS). Three different surfactants were selected to be incorporated into the amorphous solid dispersions of GF/ HPMCAS which are the anionic sodium dodecyl sulfate (SDS), the cationic dodecyletrimethylammonium bromide (DTAB) and the non-ionic pluronic (F127) (Figure 1). The rationale for selecting those surfactants is based on that SDS and DTAB have similar length of carbon chain (12 carbons) with relatively comparable critical micellar concentration (CMC). Pluronic F127 is a non-ionic surfactant and was selected to compare the impact of charge existence on the interaction with GF and acidic HPMCAS. In addition, these surfactants vary in terms of the critical micellar concentration (CMC) exhibiting a range between 0.3 to 15 mM [15-17]. This variation in the CMC provides additional factor for comparing the impact on solubility and the possible involvement of micellar solubilization in polymer-surfactants interactions. The mass ratio of the surfactants was varied between 1 to 5% so that to cover a range of concentrations across the CMC. These surfactants are commonly used excipients for pharmaceutical applications hence there is a need to understand their impact on drug-polymer interactions.

Figure 1: The chemical structures of griseofulvin, HPMCAS and surfactants.

Experimental section

Materials

GF was purchased from Sigma-Aldrich (Dorset, UK) and HPMCAS obtained from Shin-Etsu chemical (Tokyo, Japan). Sodium dodecyl sulfate (SDS, 99% purity), Dodecyletrimethylammonium bromide (DTAB, $\geq 98\%$ purity) and pluronic (F127) were obtained from Sigma- Aldrich (Dorset, UK). Acetone and NaOH pellets were purchased from VWR International LTD (UK), and sodium dihydrogen orthophosphate purchased from Fisher Scientific (Loughborough, UK). All chemicals were used without further purification.

Preparation of Physical Mixtures

Physical mixtures of varying GF:HPMCAS weight ratios which weighed a total of 1g were prepared by the method of trituration using a pestle and mortar for 10 minutes (Table 1). The first set of physical mixtures acted as the control for the study containing no added surfactant. The remainder of the physical mixtures were made up using the same ratios and took into account the

added surfactant SDS (1%, 2.5% and 5%) and Pluronic F-127 (1%, 2.5% and 5%) and DTAB (1%, 2.5% and 5%).

The size of the particles (physical mixtures) was controlled using sieving so that a narrow particle size distribution was chosen (40-90 μm). This step is necessary to conduct DSC studies that were needed for the application of the Flory-Huggins model. Thus, the onsets of the melting peaks obtained from DSC measurements correspond to the interaction between the API and the polymer rather than due to different particles sizes of the physical mixtures.

Preparation of GF-HPMCAS and GF-HPMCAS-surfactants solid dispersions

Binary solid dispersions consisting of GF and HPMCAS were prepared at mass ratio 50% GF. The total amount of dispersion produced was 5 g by which 2.5 g of GF was added to a 500 mL conical flask with 185 mL of acetone. The mixture was then stirred for 10 minutes until the GF had completely dissolved. 85 mL of distilled water was added to the conical flask and the solution was then stirred for further 10 minutes, followed by addition of 2.5 g of HPMCAS. The final mixture was then stirred for approximately 45 mins until the mixture was completely clear. The solution was finally spray dried to produce the solid dispersion of drug and polymer, using Niro SD-Micro spray dryer (Søborg, Denmark). This was connected to a nitrogen generator (Gateshead, UK), where the nitrogen gas was used as the chamber and atomizer gas. Parameters which were set for spray-drying were: inlet pressure temperature of 65°C, outlet temperature of 45°C, chamber gas flow of 25 kg/h, atomizer gas (nitrogen) flow of 2.5 kg/h, and a fixed nozzle diameter of 0.5 mm.

For preparing GF-HPMCAS-surfactants solid dispersions, different amounts of surfactants were used to prepare dispersions with fixed amounts of GF and HPMCAS of 50% each. 1, 2.5 and 5% of each surfactant was used to prepare these dispersions with 50% GF and 50% HPMCAS. The same procedure was carried out for each percentage of surfactant, for SDS, DTAB and F127. Similar spray drying conditions were used to prepare the GF-HPMCAS-surfactants. The outlet temperature was significantly below the T_g of the particles hence the impact of preparation method on crystallization was minimal.

Thermal analysis of prepared solid dispersions

Differential scanning calorimetry (DSC) was conducted on the prepared solid dispersions, which consisted of GF-HPMCAS and GF-HPMCAS- surfactants, using DSC 2920 Modulates DSC (TA instrument, UK). 5-10 mg of samples were accurately weighed into an aluminium pan, and then

hermitically crimped. The method used to measure the glass transition temperature of solid dispersions were set at a heating rate of 10°C/min using 20mL/min N₂ purge gas, and using empty pan as the reference. Indium was used as a calibrant which measured an onset melting point of 156.6°C.

Measurement of melting point depression of physical mixtures

5-10 mg of a sample of each physical mixture containing GF and HPMCAS alone and those which contained surfactants were weighed accurately in an aluminium pan and hermitically sealed. The method used to measure the onset of melting was first to equilibrate at 80°C, then keep it isothermal for 10 minutes, and finally to ramp at 5°C/min to 245°C, with an empty pan used as a reference. All measurements were done in triplicates and the average and standard deviation values were calculated.

Saturation solubility measurements

Accurately weighed samples which contained amount equivalent to 5 mg of GF were added to microcentrifuge tubes. 1 mL of phosphate buffer solution (pH 6.8) was added into each of the microcentrifuge tubes. The tubes were then placed on a Stuart® SB2 mechanical mixer (Staffordshire, UK) for 72 hours. The tubes were centrifuged using Heraeus Biofuge Pico (Germany) at 13,000 rpm for 10 minutes. The supernatant was then separated to measure absorbance using Elmer Perkins UV spectrophotometer (Cambridgeshire, UK) at 295 nm.

Thermogravimetric analysis (TGA)

Residual solvent content was analysed using a Perkin Elmer thermogravimetric analyzer TGA 6 with Pyris 6 TGA software (Perkin Elmer Corporation). Nitrogen was used as the purge gas at 20 mL/min, and each sample was heated at 10°C/min from 20°C to 200°C. All measurements were repeated in triplicates and the average and standard deviation values were calculated.

Fourier Transform Infrared (FTIR)

Infrared spectra were obtained from a Nicolet Nextus 470 FTIR spectrometer, Thermo Electron Corporation (Massachusetts, USA) which was equipped with a KBr beam splitter. An attenuated total reflectance accessory was used to obtain the spectra, in the form of a single reflection

bounce diamond crystal, Golden Gate accessory). A total of 64 scans were collected for each sample with a resolution of 4 cm^{-1} using a frequency range of 4000 cm^{-1} to 550 cm^{-1} .

Measurement of particle size distribution

The size distribution of particles in the physical mixtures and solid dispersions was assessed using Malvern Mastersizer (Worcestershire, UK). Phosphate buffer solution (pH 6.8) was used to disperse the particles. Ten consecutive repeat measurements were carried out, each with 2500 sweeps and an interference of 20%.

Scanning Electron Microscopy (SEM)

The sample particles were fixed on to the surface of a conductive double-sided carbon adhesive, attached to an aluminium stub. The prepared samples were sputter coated with gold, for 3 minutes at 30 mA, using Emitech K550 (Ashford, UK). The micrographs were collected using a Philips FEI KL (Eindhoven, Netherlands).

Statistical analysis

Statistical analysis of the data was carried out by one-way analysis of variance (ANOVA) with Tukey's multiple comparison tests at a significance level of $p < 0.05$ using SPSS 22 software (IBM).

Results

Glass transition temperature and thermogravimetric analysis

The glass transition temperature (T_g) is a second order transition event that occurs when the amorphous glassy state changes to the less viscous supercooled liquid. The non-equilibrium nature of glassy state will encourage higher molecular mobility leading to relaxation and loss of excess configurational energy. The impact of adding the surfactants was evaluated by measuring the T_g of the solid dispersions. Lowering in the T_g was observed when the surfactants were incorporated into the solid dispersions. As can be seen in Figure 2, the T_g values have been reduced significantly when surfactants were added into the solid dispersions with maximum lowering was observed when F127 was incorporated. Insignificant statistical difference between different ratios was observed for dispersions containing SDS. A statistical difference was only seen for dispersions containing 5% DTAB compared with the 1 and 2.5% while all ratios of F127 showed significant difference. The average T_g values were significantly different between F127 and SDS/DTAB while there was no statistical difference between the

average T_g values for DTAB and SDS dispersions. One possible explanation for the significant reduction in the T_g is the presence of residual solvents. Hence, to examine this effect, thermogravimetric analysis (TGA) was performed.

Figure 2: (a) Typical DSC thermogram showing different thermal events when heating GF: HPMCAS solid dispersions and (b) glass transition temperature values (T_g) for spray dried amorphous solid dispersions prepared using GF: HPMCAS (50%:50%) containing different ratios of the surfactants (SDS, DTAB, F127). The dotted line shows the T_g for the GF/HPMCAS amorphous solid dispersion without surfactants.

As can be seen in Table 2, the amount of residual solvent did not differ significantly between the various solid dispersions with an average residual solvent content of around 1%. Hence, the lower T_g values could not be attributed to the presence of solvent but rather due to the effect of the surfactant on the drug-polymer matrix.

Measurement of melting point (T_m) and heat of fusion of physical mixtures and prediction of thermodynamics of mixing

Figure 3 shows the onset of melting peak and heat of fusion of physical mixtures. As can be seen, overall trend showed reduction in both melting point onset and heat of fusion. There were differences in the extent of this lowering by which SDS containing mixtures were associated with the sharpest decline in the melting point followed by DTAB whilst minor differences were observed for mixtures that contained F127 compared to mixtures without surfactants. The heat of fusion which represents the total enthalpy of the crystalline lattice did not follow the same trend by which F127 mixtures showed the sharpest reduction compared to other mixtures. It is worth mentioning that shifts in thermal events often reflects good miscibility between the drug and the polymer. These can also happen when non uniform crystalline domains form during recrystallization. On the other hand, there are examples in the literature where no differences in terms of the melting point depression could be observed [18]. Due to thermal degradation of some mixtures, measurement of the heat of fusion was not possible.

Figure 3: (a) onset of melting point of GF in physical mixtures of GF: HPMCAS containing varied ratios of the surfactants and (b) heat of fusion of the physical mixtures. Some physical mixtures such as SDS mixtures were not possible to measure due to thermal degradation.

278

279 Flory-Huggins model was used to analyse the shifts in the heat of fusion and melting point
 280 depression of physical mixtures. This modified model takes into account the molecular volume
 281 of the drug in relation to the polymer. The polymer is theoretically divided into voids that are
 282 equivalent to the molecular volume of the drug. Hence, the incidence of interactions between
 283 the polymer and the drug are normalized thus the smaller the molecular volume (and therefore
 284 the voids) of the drug, the highest is the entropy effect. This positive impact on free energy of
 285 mixing is counterbalanced by the enthalpy of mixing which is accounted for through the Flory-
 286 Huggins interaction parameter (χ). Using thermal analysis of drug-polymer physical mixtures,
 287 this parameter can be calculated using both depression in the melting point as well as the molar
 288 heat of fusion. Despite some drawbacks associated with the use of this method, it can provide
 289 significant insight on the extent of interactions especially when similar systems are compared.

290

291 For the determination of enthalpy, entropy and energy of mixing, the Flory-Huggins model was
 292 applied [18-20]. ΔG_M is the free energy of mixing for n_{drug} and $n_{polymer}$, present at Φ_{drug} and $\Phi_{polymer}$
 293 volume fractions. The interaction parameter χ accounts for the enthalpy of mixing. It can be
 294 calculated from equation (1) and then substituted into (2) to find the free energy of mixing [18,
 295 19].

296

$$\frac{\Delta G_M}{RT} = n_{drug} \ln \Phi_{drug} + n_{polymer} \ln \Phi_{polymer} + \chi n_{drug} \Phi_{polymer} \quad (1)$$

299

$$\left(\frac{1}{T_M^{mix}} - \frac{1}{T_M^{pure}} \right) = \frac{-R}{\Delta H_{fus}} \left[\ln \Phi_{drug} + \left(1 - \frac{1}{m} \right) \Phi_{polymer} + \chi \Phi_{polymer}^2 \right] \quad (2)$$

302

303 where T_M^{mix} and T_M^{pure} are the melting temperatures of the drug in the presence of polymer and
 304 alone, respectively; ΔH_{fus} is the enthalpy of fusion of pure drug, and m is the ratio of the polymer
 305 to drug volume (calculated as molar volumes derived from true density).

306

307 As can be seen in Figure 4, the results showed that physical mixtures that contained DTAB
 308 were associated with the lowest free energy of mixing compared to other mixtures. Thermal
 309 degradation was more pronounced in SDS containing mixtures hence only 1% mixtures were
 310 analysed. There was obvious difference in the extent of mixing by which the surfactants lowered

the free energy of mixing and ultimately means the miscibility of the drug and the polymer are enhanced. Consequently, the drug-polymer miscibility was enhanced by approximately 1.3 folds when 2.5% DTAB was incorporated. This approximation is based on free energy of mixing for mixtures without surfactants of -3.1×10^{-6} J/g which was lowered to -4.4×10^{-5} J/g for DTAB mixtures. Due to thermal degradation, mixtures that contained higher ratios of the surfactant, were not possible to analyse using this method. However, assuming extrapolated effect, the drug-polymer miscibility will be enhanced by approximately 1.5-2 folds when compared to mixtures that did not contain any surfactants.

Figure 4: Flory-Huggins analysis of the thermodynamics of mixing using melting point depression of physical mixtures of GF: HPMCAS and incorporating different ratios of the surfactants. Some surfactant ratios were not possible to measure due to thermal degradation.

Assessment of GF-HPMCAS miscibility using reduced onset of crystallization of amorphous solid dispersions

When heating the amorphous dispersion, the drug/ polymer molecules will gain sufficient molecular mobility that will cause the solid dispersion to move to the rubbery state. Once the dispersion is in the rubbery state, the molecules will move at significantly faster rate allowing them to rearrange and recrystallize in the most stable crystalline structure. Additional heating will lead to fusion event and liberation from the solid state. The onset of these events can be used as a measure of drug miscibility in the solid dispersion. Here we use a combination of analytical tools to assess the extent of drug-polymer miscibility which are melting point depression and reduced onset of crystallization.

While the shifted onset of recrystallization temperature (T_c) can indicate altered kinetics for recrystallization, the ratio between the T_c , T_g and T_m will be more precise method to predict miscibility. The rationale for using this ratio is to establish a common scale for different dispersions regardless of the measurement conditions. As such the minimum point on the scale is the T_g and the maximum is T_m . This ratio can be described as the ratio of the difference between onset of recrystallization temperature (T_c) and T_g to the difference between melting point onset (T_m) and T_g [21].

$$R_c = \frac{T_c - T_g}{T_m - T_g}$$

Depending on the onset values of T_m , T_g and T_c , the ratio can be used to predict likelihood for spontaneous recrystallization. Lower ratios implicate faster rate of recrystallization of amorphous materials [22].

As can be seen in Figure 5, reduced recrystallization was different among prepared dispersions. When compared with GF which was found to have recrystallization ratio of 0.32 [22], the prepared dispersions showed higher values. For example, SDS containing solid dispersions displayed R_c values between 0.48 to 0.58 with sharp reduction in R_c when the ratio of SDS was increased to 5%. F127 solid dispersions showed the lowest recrystallization ratios with a range between 0.44-0.46. Among the three surfactants, only DTAB solid dispersions showed positive correlation between reduced recrystallization and surfactant ratio in the solid dispersion. Overall, these results indicate that the extent of recrystallization follows the following trend SDS>DTAB>F127 at low surfactant ratios and follows the following trend DTAB>SDS>F127 at high surfactant ratios. Both DTAB and SDS solid dispersions showed higher ratios than the spray dried amorphous solid dispersion prepared without surfactants. Hence, these results suggest that incorporating DTAB and SDS (within tested range) may increase physical stability of the amorphous form. It is worth mentioning that the onset values were used to perform the analysis; all samples did not exhibit thermal degradation within the onset melting temperature.

Figure 5: Reduced recrystallization of spray dried amorphous solid dispersions of GF: HPMCAS (50%:50%) containing varied ratios of the surfactants. The x symbol represents the value for spray dried amorphous solid dispersion without surfactants.

Pearson correlation coefficient (r) values for linear trends in Figure 5 were calculated and showed that DTAB had r value of 0.84 while SDS and F127 dispersions showed r values of -0.96 and -0.98, respectively. This analysis indicates strong linear relationship between the surfactant ratio and the reduced recrystallization values. The positive r indicates that increasing DTAB ratio in the dispersion increased R_c while the opposite trend was correct for SDS and F127.

Aqueous saturated solubility measurements

378 The saturation solubility of spray dried amorphous solid dispersions and corresponding physical
379 mixtures was measured in phosphate buffer (pH 6.8). As can be seen in Figure 6, the solid
380 dispersions of GF and HPMCAS with SDS exhibited higher GF aqueous solubilities than the
381 corresponding physical mixtures with solubilities in the range of 101-121 $\mu\text{g/mL}$. This value was
382 higher than the solid dispersions of GF and HPMCAS prepared in the absence of surfactant that
383 showed solubility of 88 $\mu\text{g/mL}$. On the other hand, solid dispersions of GF and HPMCAS with
384 F127 showed solubility results comparable to or slightly higher than the corresponding physical
385 mixtures. Increasing the ratio of F127 from 1% to 5% led to lower solubility values of 115 and
386 84 $\mu\text{g/mL}$, respectively. Solid dispersions of GF and HPMCAS with DTAB showed even lower
387 solubility values than SDS and F127 containing solid dispersions. Increasing the ratio of DTAB
388 from 1% to 5% has led to lower solubility values of 74 and 42 $\mu\text{g/mL}$, respectively.

389

390 **Figure 6:** Saturated aqueous solubility measurements of spray dried amorphous solid
391 dispersions (SD) of GF: HPMCAS (50%: 50%) containing varied ratios of surfactants and
392 compared with corresponding physical mixtures (PM).

393

394 Analysis of surfactants micellar solutions showed that SDS achieved significant enhancement in
395 GF solubility (Figure 7). The micellar solutions were prepared using mass ratio in distilled water
396 via adding excess amount of GF to determine saturation solubility. Saturation solubility
397 exceeded 6mg/mL for SDS while for DTAB was around 1.6mg/L and 0.1 mg/L for F127. It is
398 interesting to observe that these trends did not correlate with GF solubility when it was
399 dissolved as a solid dispersion. It is evident from Figure 6 that the cationic DTAB showed
400 reduced solubility compared with SDS and F127 which could be attributed to forming ionic
401 interactions with the acidic HPMCAS. It is also interesting to see that F127 solid dispersions
402 displayed similar solubility to the micellar solutions despite that the F127 content is significantly
403 less in the solid dispersions. When comparing the critical micellar concentrations (CMC), the
404 following trends can be seen DTAB>SDS>F127 (DTAB 15 mM, SDS 8.25 mM, F127 0.357 mM)
405 [15-17]. Hence, it is possible that the low CMC of F127 meant that micelles could be present
406 when the solid dispersions were dissolved.

407

408 **Figure 7:** Saturated solubility of GF in micellar solutions of different w/v% ratios of SDS, DTAB,
409 F127.

410

411

Correlation between predicted and experimental solubility

Originally used to calculate solubility ratio of glucose glass to α -glucose crystals, equation 4 has been widely used to predict solubility ratio between the amorphous/crystalline forms ($\frac{\sigma_a}{\sigma_c}$) [23],

$$\Delta G_{c \rightarrow a} = -RT \ln \frac{\sigma_a}{\sigma_c} (1)$$

(4)

Where R is the gas constant and $\Delta G_{c \rightarrow a}$ is the free energy changes associated with the conversion of the amorphous to the crystalline form.

Prediction of the solubility ratio is based on the assumption that the additional free energy of the amorphous form is proportional to the increase in kinetic energy leading to enhanced solubility. A possible theoretical approach to predict the difference in solubility of the amorphous as compared to the crystalline form is via the use of Hoffman's equation to calculate the total free energy change associated from the crystalline to the amorphous form ($\Delta G_{c \rightarrow a}$) [24],

$$\Delta G_{c \rightarrow a} = \frac{\Delta H \cdot T (T_m - T)}{T_m^2}$$

(5)

By which ΔH is the enthalpy of fusion and T being the temperature of interest.

As can be seen in Figure 8, the solubility ratio of GF at 298.15 K is approximately 65 with configurational free energy of 10.4 kJ/mol. The rapid recrystallization of GF makes it difficult to experimentally determine the amorphous form solubility hence this method represents a good approximation of solubility enhancement of fully amorphous GF. As can be seen, the configurational free energy decreased with increasing the temperature indicating that glass GF will exhibit maximum solubility around 298.15 K. This value does not take in consideration any kinetic contributions to increasing the solubility but is purely based on free energy excess of the amorphous form.

Figure 8: Solubility ratio (amorphous/crystalline) of GF versus configurational energy.

Experimental solubility measurements of amorphous solid dispersions were used to calculate the solubility ratios relative to the solubility of crystalline GF (Figure 9). As can be seen, the solubility ratio of the amorphous solid dispersions (without surfactants) was found to be 8.8. This is significantly lower than the expected value for amorphous GF which may indicate possible recrystallization during dissolution. We have shown before that amorphous solid dispersions exhibited time dependent solubility by which a peak concentration was observed after 1 hour [25]. The assumption of amorphous form higher solubility should therefore be evaluated within the same time frame. Maintaining GF as amorphous for 72 hours is not possible as it tends to crystallize within hours when stored at dry conditions. Practically, solubility of amorphous GF cannot be determined accurately because recrystallization happens so fast which makes determination of this value largely hypothetical. The results show positive impact when SDS was incorporated with a solubility ratio range between 10-12. The lower solubility of DTAB solid dispersion can be clearly seen with solubility ratios reaching 4 indicating that the drug solubility was halved when compared with the dispersions that did not contain any surfactants. Opposite to SDS dispersions, F127 initially enhanced the solubility ratio but was decreased when the F127 ratio was increased to 5%.

Figure 9: Experimental solubility ratios of GF from amorphous solid dispersions compared with the experimentally determined solubility of crystalline GF.

As can be seen in Figure 10, reduced recrystallization was lowest for F127 containing solid dispersions. When the ratio of the F127 was increased from 1% to 5%, reduced recrystallization decreased which was also associated with lower solubility. This trend was reversed in the case of DTAB solid dispersions which was associated with reduced solubility values. SDS solid dispersion showed slightly variable solubility ratio which was affected to less extent by R_c . These results suggest that the surfactants may affect nucleation and possibly crystal growth upon exposure to aqueous media. Furthermore, solubility differences between physical mixtures and spray dried solid dispersions reflect key role for the amorphous form and the molecular interactions with the polymer.

Figure 10: Reduced crystallization of spray dried amorphous solid dispersions against experimental solubility ratio.

Spectroscopic analysis of solid dispersions

FTIR was carried out to identify if there was a possible hydrogen bonding between the GF and HPMCAS, and to assess whether the presence of surfactants affects this interaction. The absorbances between 1750 and 1550 cm^{-1} correspond to the C=O stretch of the benzofuran ring and cyclohexene, and C=C stretch of the cyclic rings of the structure shown in Figure 11. GF has two peaks which correspond to the two carbonyl groups, so there are two distinctive peaks; the first at 1712 cm^{-1} which corresponds to stretching of the C=O in the benzofuran ring and the second peak at 1662 cm^{-1} which corresponds to C=O of cyclohexene. It was shown before that the presence of HPMCAS caused a broadening of carbonyl peak at 1662 cm^{-1} which is an indication of hydrogen bonding been present which results in a shift of peak to the right to a lower frequency [7]. Presence of amorphous GF formation can be confirmed by the disappearance of peaks at 1220, 1350 and 1580 cm^{-1} . Overall, the presence of the surfactants did not affect the peaks positions, nor the broadening seen in the GF/ HPMCAS solid dispersions indicating no alteration of polarity around aforementioned groups.

Figure 11: FTIR spectra showing (a) GF, HPMCAS, GF: HPMCAS solid dispersion (50%:50%) (SD) and corresponding physical mixture (PM). The arrows indicate peaks that disappeared when amorphous GF was formed and (b) SD of GF: HPMCAS (50%:50%) with 5% surfactants showing no difference in peaks positions compared with (GF: HPMCAS) SD.

Particle size and morphology analysis of solid dispersions

Particle size analysis showed that the GF: HPMCAS physical mixtures prepared with different surfactants ratios had a particle size range between 10-20 μm (Figure 12). It is interesting to observe that surfactants caused larger particle size distribution when compared with the GF:HPMCAS mixtures. Such behaviour may suggest bridging the polymer chain through the surfactant forming larger aggregates. The trend seemed stronger in the following order SDS>DTAB>F127 reflecting differences in the intermolecular interactions promoting aggregate formation. Opposite to this trend is the particle size analysis of spray dried solid dispersions which showed that F127 particles were larger than SDS and DTAB dispersions.

Figure 12: Particle size analysis of GF: HPMCAS physical mixtures prepared with different surfactants ratios. Also shown is the particle size analysis of amorphous solid dispersions of GF: HPMCAS (50%:50%) prepared with different surfactants ratios.

511

512 To understand whether the trends observed above were due to the exposure to aqueous media
513 which could have induced aggregations, scanning electron microscopy images were used to analyse
514 morphology and particle size in the solid state (Figure 13). As can be seen, the particles were
515 spherical with particle size distribution smaller for F127 solid dispersions suggesting that the
516 particle size growth was promoted by the aqueous media used when measuring the particles size.

517

518 **Figure 13:** Scanning electron microscopy showing spray dried amorphous solid dispersions of
519 GF: HPMCAS (50%:50%) with (a) 2.5% DTAB, (b) 2.5% F127, (c) 2.5% SDS and (d) no
520 surfactants.

521

522

523 Discussion

524 The results presented in this research showed that surfactants can enhance the solid state
525 miscibility of the model drug GF with HPMCAS. The enhanced solid state miscibility can be
526 attributed to lowering the heat of mixing which can interfere with the extent of mixing. The extent
527 of this lowering was found to be highest when DTAB was used. After spray drying, the drug-
528 polymer interactions are expected to mirror the interactions observed in the melted physical
529 mixtures. The main difference would be the impact of the solvent on whether it can hinder or limit
530 intermolecular interactions. As was seen, it was possible to see a correlation between the
531 reduced crystallization parameter which represents the difference in glass transition,
532 crystallization and melting temperatures. It is expected that enhanced solid state miscibility will
533 be translated as enhanced saturated solubility. This expectation is based on the fact that
534 HPMCAS is a hydrophilic polymer and enhanced miscibility is a result of increased intermolecular
535 contacts with the drug and therefore improve the saturated solubility. When surfactants were
536 incorporated into the solid dispersions, the solubility decreased with a trend that suggests lack of
537 micellar solubilization. This conclusion was based on comparison with micellar solubility of GF
538 suggesting that the surfactants chains were molecularly associated with HPMCAS.

539

540 The lowest solubility was found in DTAB solid dispersions which could potentially be attributed to
541 electrostatic interactions with HPMCAS. There were no signs of disruption of the intermolecular
542 hydrogen bonding of GF with HPMCAS as evident from FTIR analysis hence all events observed
543 above can be attributed to exposure to the aqueous media. Based on particle size analysis, a
544 possible explanation would be that the growth of the particle size can be due to gelation

happening during the dissolution process which was particularly promoted by the polymeric nature of F127. The intermolecular interactions were clearly very different from the physical mixtures reflected in different particles size distribution. Overall, these data showed that the role of surfactant is a complex role and can significantly be altered upon exposure to the dissolution media.

Miscibility in the solid state can certainly be enhanced but that depends on the nature of intermolecular interactions. Nevertheless, solid state miscibility may not be a prerequisite for a better dissolution as the presence of water can promote particles aggregation. The type of surfactant is critical for enhanced miscibility of the drug with the polymer; hence screening can be used to select the optimum surfactant ratio while preventing possible recrystallization upon dissolution. While there is no evidence of forming localised regions of amorphous drug within surfactant aggregates, lowered saturated solubility cannot solely be attributed to recrystallization of the amorphous drug. Hence, it is possible that the drug is localized within micro amorphous domains prior to dissolution resembling micellar structures. These structures remain hypothetical and will be the focus of future research.

Conclusions

The impact of incorporating surfactants on thermodynamic parameters was assessed. Overall trend showed that DTAB containing solid dispersions had highest miscibility when compared with other dispersions. However, when comparing saturated solubility, the impact on solubility was reversed. The findings of this work highlight, for the first-time, potential correlation between phase transition temperatures and drug polymer miscibility which can be used to design amorphous dispersions with enhanced properties. While there was a positive impact in terms of enhancing drug-polymer miscibility, the impact on saturation solubility requires further investigation.

Conflicts of interest

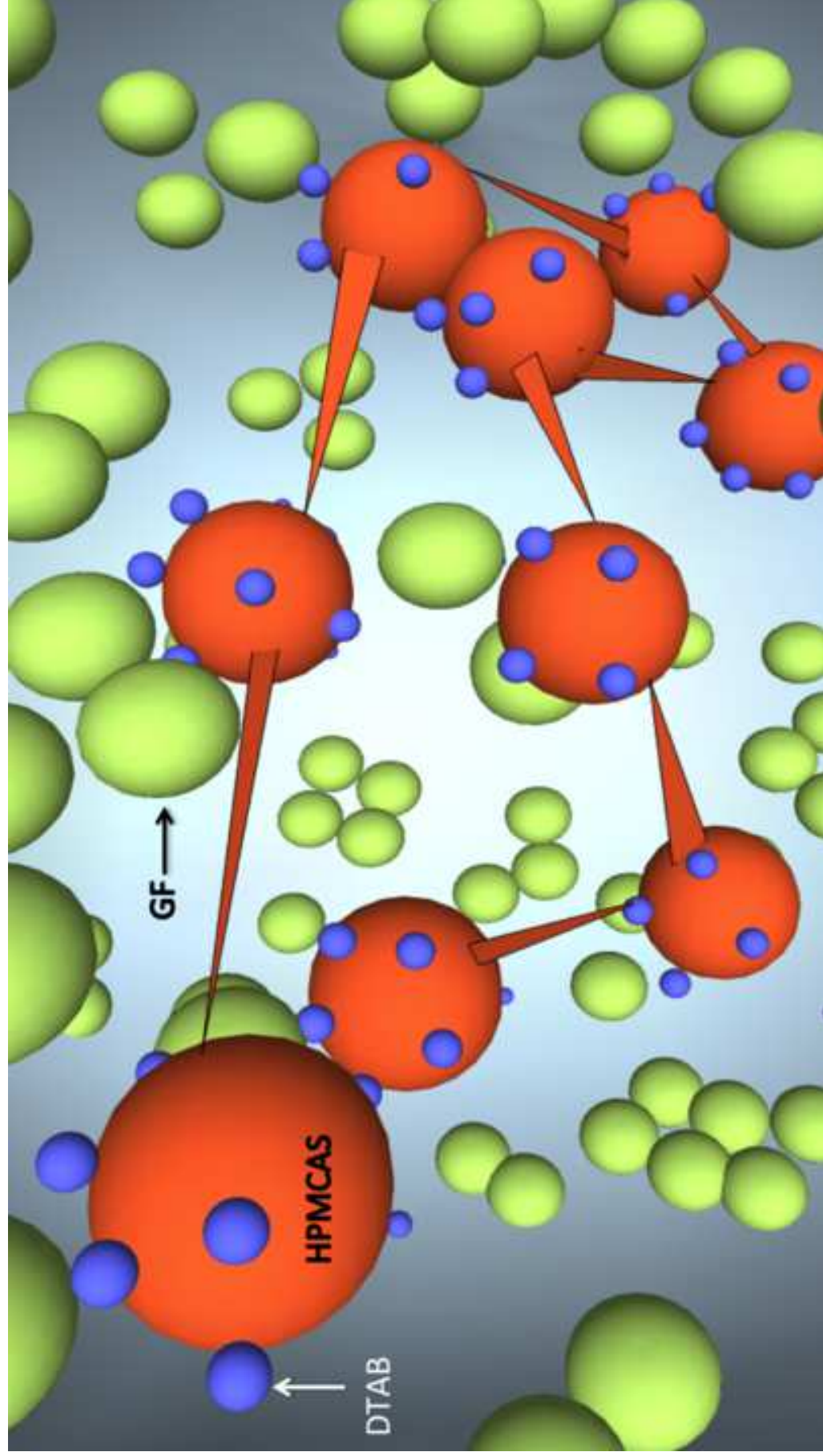
There are no conflicts to declare.

Acknowledgements

The authors would like to thank the Chemical Analysis Facility at the University of Reading for providing essential access to instruments used in this study.

580 References

- 581 [1] H.H. Tong, Z. Du, G.N. Wang, H.M. Chan, Q. Chang, L.C. Lai, A.H. Chow, Y. Zheng, Spray freeze drying with polyvinylpyrrolidone and sodium
582 caprate for improved dissolution and oral bioavailability of oleanolic acid, a BCS Class IV compound, *International journal of pharmaceutics*,
583 404 (2011) 148-158.
- 584 [2] J.A. Baird, L.S. Taylor, Evaluation of amorphous solid dispersion properties using thermal analysis techniques, *Adv Drug Deliv Rev*, (2011).
- 585 [3] B. Li, S. Konecke, L.A. Wegiel, L.S. Taylor, K.J. Edgar, Both solubility and chemical stability of curcumin are enhanced by solid dispersion in
586 cellulose derivative matrices, *Carbohydrate polymers*, 98 (2013) 1108-1116.
- 587 [4] P. Srinarong, H. de Waard, H.W. Frijlink, W. Hinrichs, Improved dissolution behavior of lipophilic drugs by solid dispersions: the production
588 process as starting point for formulation considerations, *Expert Opin Drug Deliv*, 8 (2011) 1121-1140.
- 589 [5] D. Horter, J.B. Dressman, Influence of physicochemical properties on dissolution of drugs in the gastrointestinal tract, *Adv Drug Deliv Rev*,
590 46 (2001) 75-87.
- 591 [6] R. Laitinen, E. Suihko, M. Bjorkqvist, J. Riikonen, V.P. Lehto, K. Jarvinen, J. Ketolainen, Perphenazine solid dispersions for orally fast-
592 disintegrating tablets: physical stability and formulation, *Drug Dev Ind Pharm*, 36 (2010) 601-613.
- 593 [7] H. Al-Obaidi, G. Buckton, Evaluation of griseofulvin binary and ternary solid dispersions with HPMCAS, *AAPS PharmSciTech*, 10 (2009)
594 1172-1177.
- 595 [8] J.A. Baird, B. Van Eerdenbrugh, L.S. Taylor, A classification system to assess the crystallization tendency of organic molecules from
596 undercooled melts, *Journal of pharmaceutical sciences*, 99 (2010) 3787-3806.
- 597 [9] H. Al-Obaidi, M.J. Lawrence, S. Shah, H. Moghul, N. Al-Saden, F. Bari, Effect of drug-polymer interactions on the aqueous solubility of
598 milled solid dispersions, *International journal of pharmaceutics*, 446 (2013) 100-105.
- 599 [10] M. Aldén, M. Lydén, J. Tegenfeldt, Effect of counterions on the interactions in solid dispersions between polyethylene glycol, griseofulvin
600 and alkali dodecyl sulphates, *Int. J. Pharm.*, 110 (1994) 267-276.
- 601 [11] M. Wulff, M. Aldén, D.Q.M. Craig, An investigation into the critical surfactant concentration for solid solubility of hydrophobic drug in
602 different polyethylene glycols, *Int. J. Pharm.*, 142 (1996) 189-198.
- 603 [12] S. Sheokand, J. Sharma, A.K. Bansal, Effect of surfactants on the molecular mobility and crystallization kinetics of hesperetin,
604 *CrystEngComm*, 21 (2019) 3788-3797.
- 605 [13] T.M. Deshpande, H. Shi, J. Pietryka, S.W. Hoag, A. Medek, Investigation of Polymer/Surfactant Interactions and Their Impact on
606 Itraconazole Solubility and Precipitation Kinetics for Developing Spray-Dried Amorphous Solid Dispersions, *Mol Pharmaceut*, 15 (2018) 962-
607 974.
- 608 [14] H. Al-Obaidi, M.J. Lawrence, G. Buckton, Atypical effects of incorporated surfactants on stability and dissolution properties of amorphous
609 polymeric dispersions, *The Journal of pharmacy and pharmacology*, 68 (2016) 1373-1383.
- 610 [15] V. Peyre, S. Bouguerra, F. Testard, Micellization of dodecyltrimethylammonium bromide in water-dimethylsulfoxide mixtures: a multi-
611 length scale approach in a model system, *Journal of colloid and interface science*, 389 (2013) 164-174.
- 612 [16] Y. Moroi, K. Motomura, R. Matuura, The critical micelle concentration of sodium dodecyl sulfate-bivalent metal dodecyl sulfate mixtures
613 in aqueous solutions, *J Colloid Interface Sci*, 46 (1974) 111-117.
- 614 [17] L.M.U. Dutra, M.E.N.P. Ribeiro, I.M. Cavalcante, D.H.A.d. Brito, L.d.M. Semião, R.F.d. Silva, P.B.A. Fechine, S.G. Yeates, N.M.P.S. Ricardo,
615 Binary mixture micellar systems of F127 and P123 for griseofulvin solubilisation, *Polímeros*, 25 (2015) 433-439.
- 616 [18] H. Al-Obaidi, P. Ke, S. Brocchini, G. Buckton, Characterization and stability of ternary solid dispersions with PVP and PHPMA, *International*
617 *journal of pharmaceutics*, 419 (2011) 20-27.
- 618 [19] P.J. Marsac, H. Konno, A.C. Rumondor, L.S. Taylor, Recrystallization of nifedipine and felodipine from amorphous molecular level solid
619 dispersions containing poly(vinylpyrrolidone) and sorbed water, *Pharmaceutical research*, 25 (2008) 647-656.
- 620 [20] J. Djuris, I. Nikolakis, S. Ibric, Z. Djuric, K. Kachrimanis, Preparation of carbamazepine-Soluplus solid dispersions by hot-melt extrusion,
621 and prediction of drug-polymer miscibility by thermodynamic model fitting, *European journal of pharmaceutics and biopharmaceutics* :
622 official journal of Arbeitsgemeinschaft fur Pharmazeutische Verfahrenstechnik e.V, 84 (2013) 228-237.
- 623 [21] D. Zhou, G.G. Zhang, D. Law, D.J. Grant, E.A. Schmitt, Physical stability of amorphous pharmaceuticals: Importance of configurational
624 thermodynamic quantities and molecular mobility, *Journal of pharmaceutical sciences*, 91 (2002) 1863-1872.
- 625 [22] P. Gupta, G. Chawla, A.K. Bansal, Physical Stability and Solubility Advantage from Amorphous Celecoxib: The Role of Thermodynamic
626 Quantities and Molecular Mobility, *Mol Pharmaceut*, 1 (2004) 406-413.
- 627 [23] G.S. Parks, L.J. Snyder, F.R. Cattoir, Studies on glass. XI. Some thermodynamic relations of glassy and alpha-crystalline glucose, *J Chem*
628 *Phys*, 2 (1934) 595-598.
- 629 [24] J.D. Hoffman, Thermodynamic driving force in nucleation and growth processes, *J Chem Phys*, 29 (1958) 1192-1193.
- 630 [25] H. Al-Obaidi, M.J. Lawrence, N. Al-Saden, P. Ke, Investigation of griseofulvin and hydroxypropylmethyl cellulose acetate succinate
631 miscibility in ball milled solid dispersions, *International journal of pharmaceutics*, 443 (2013) 95-102.



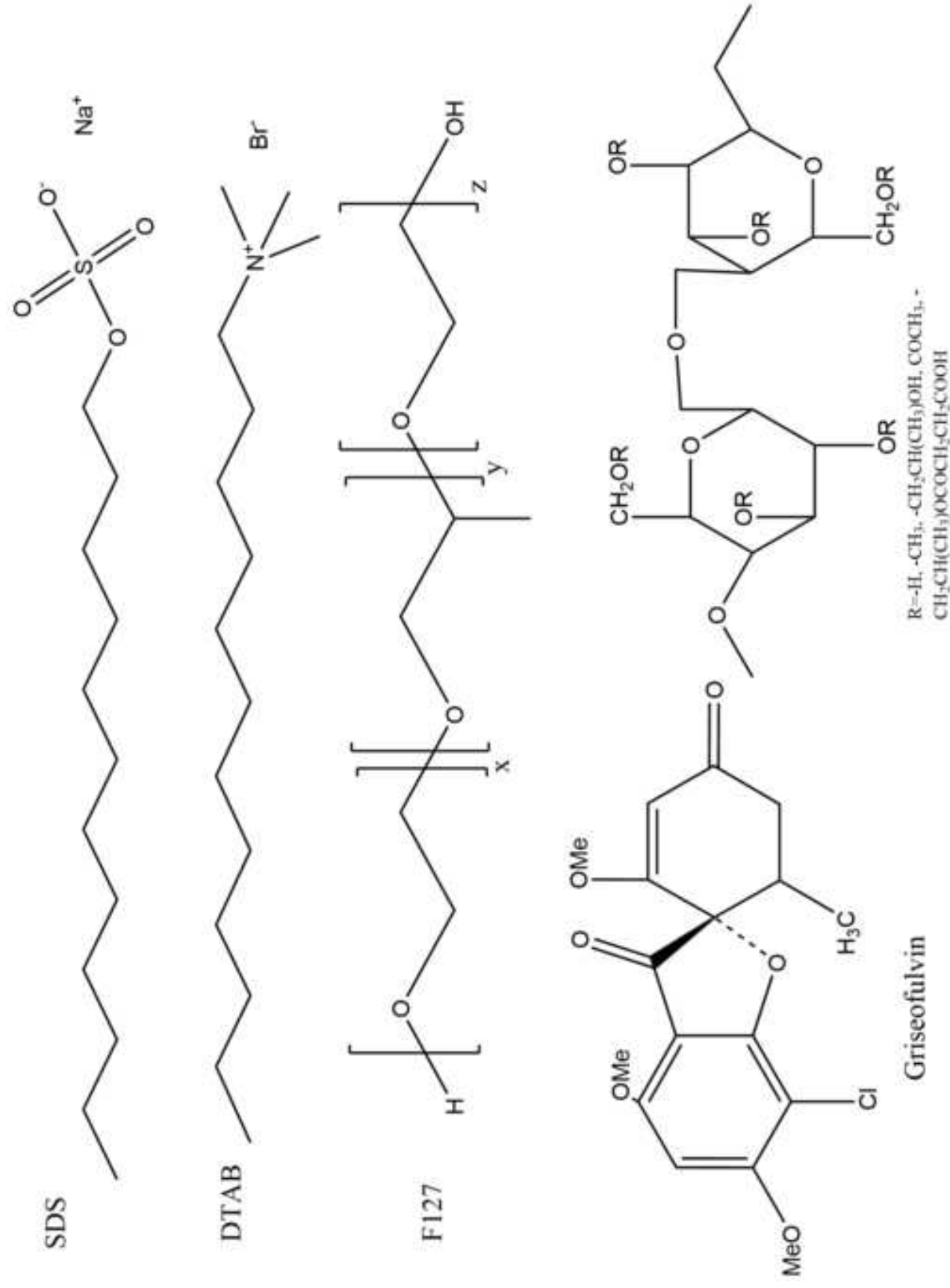


Figure 2a

[Click here to access/download;Figure;Figure 2_a.jpg](#)

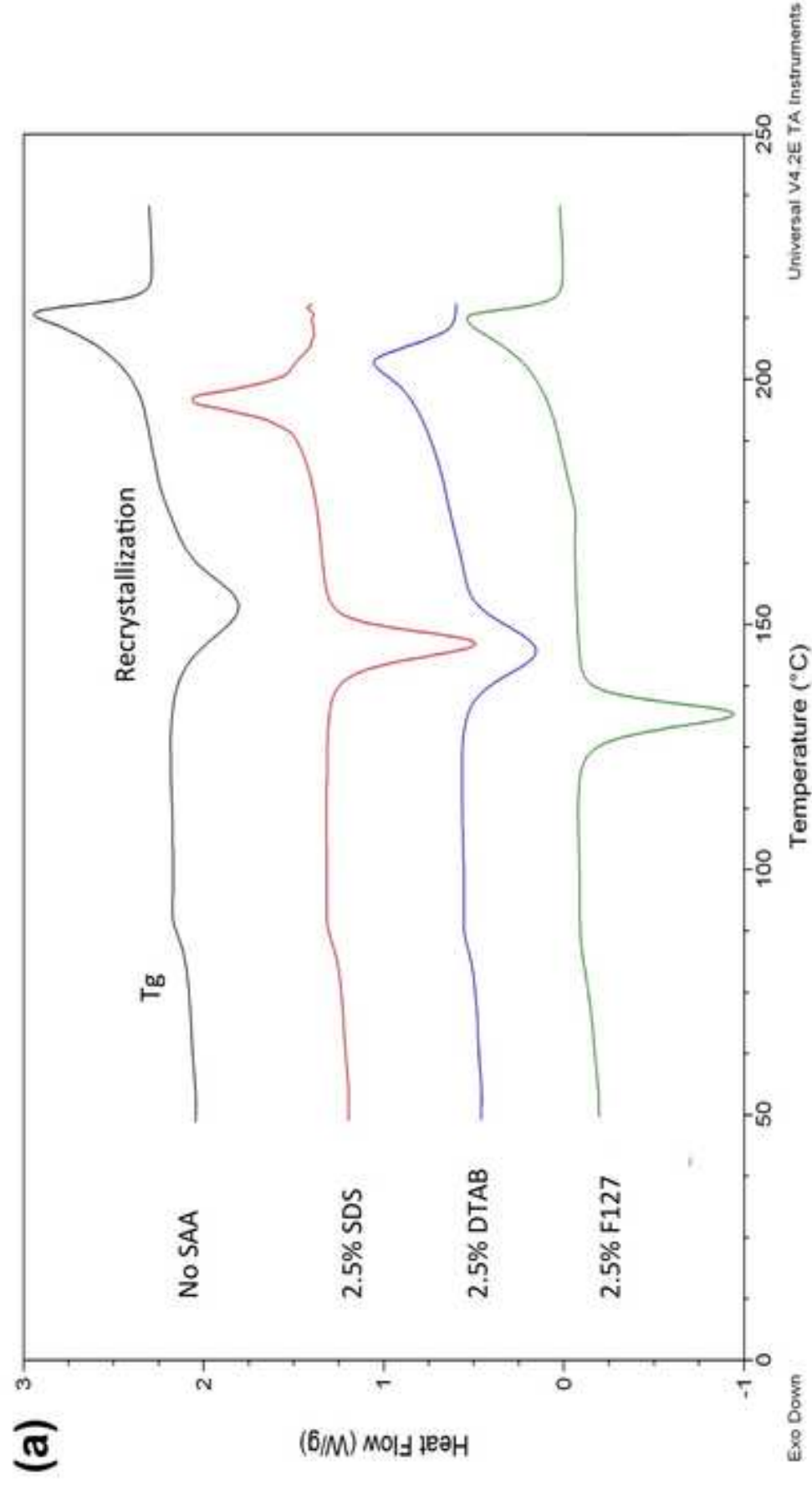


Figure 2b

[Click here to access/download;Figure;Figure 2_b.jpg](#)

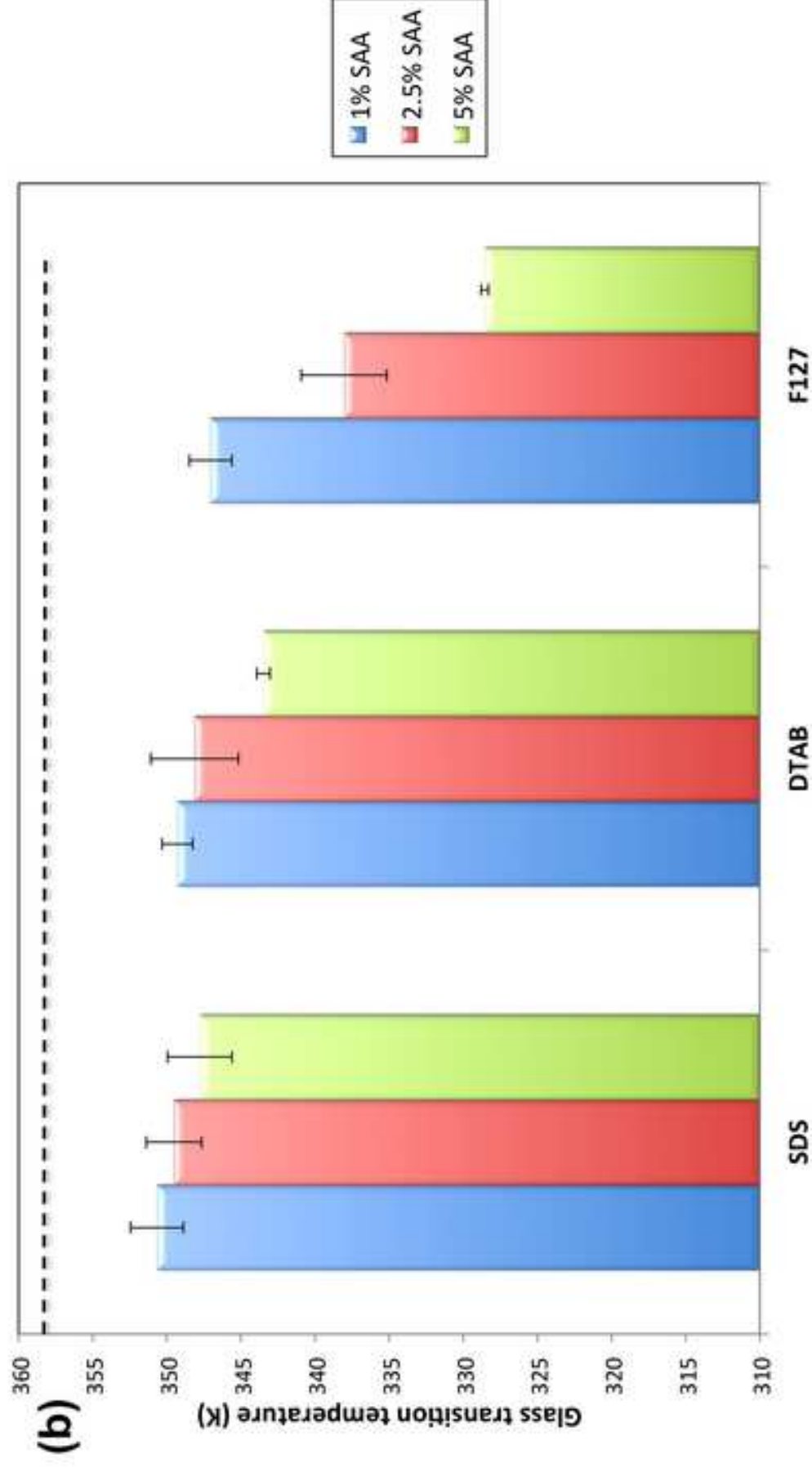
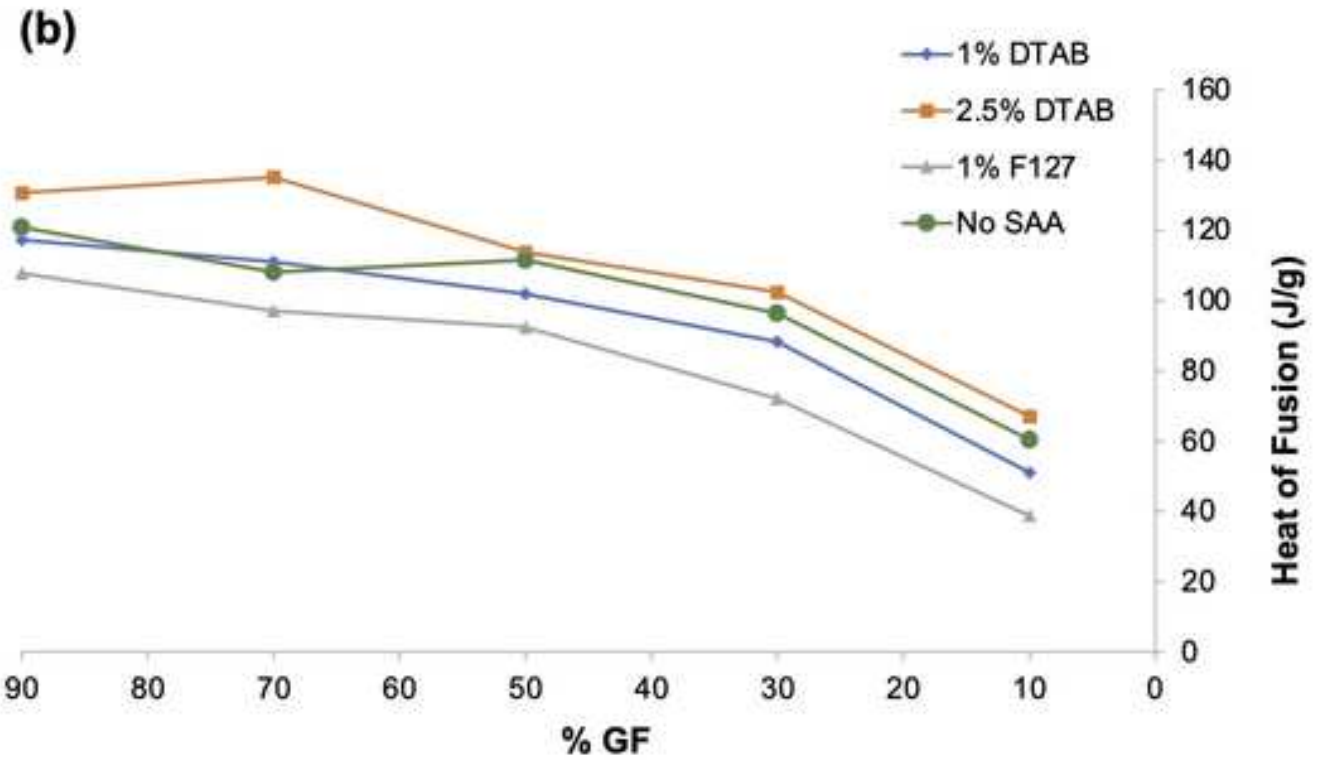
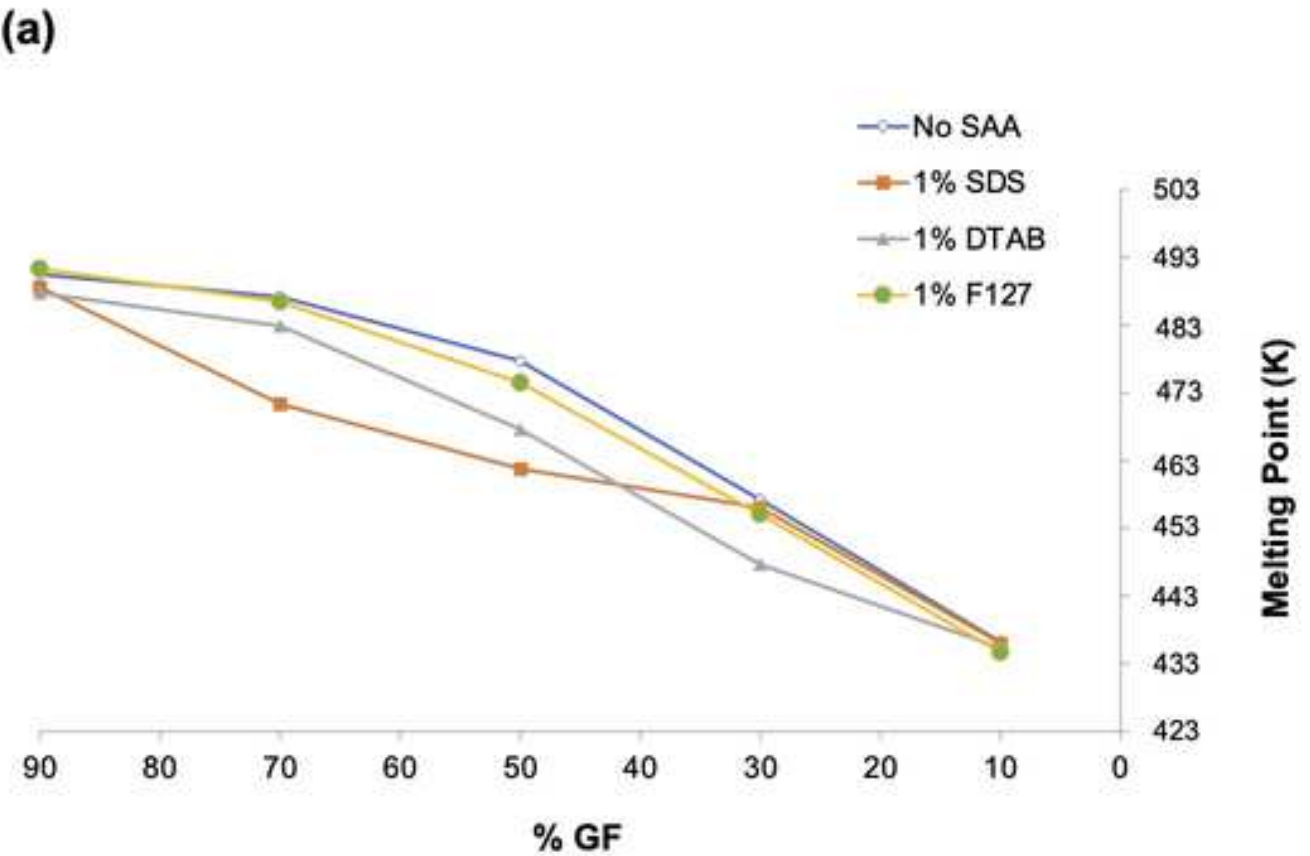


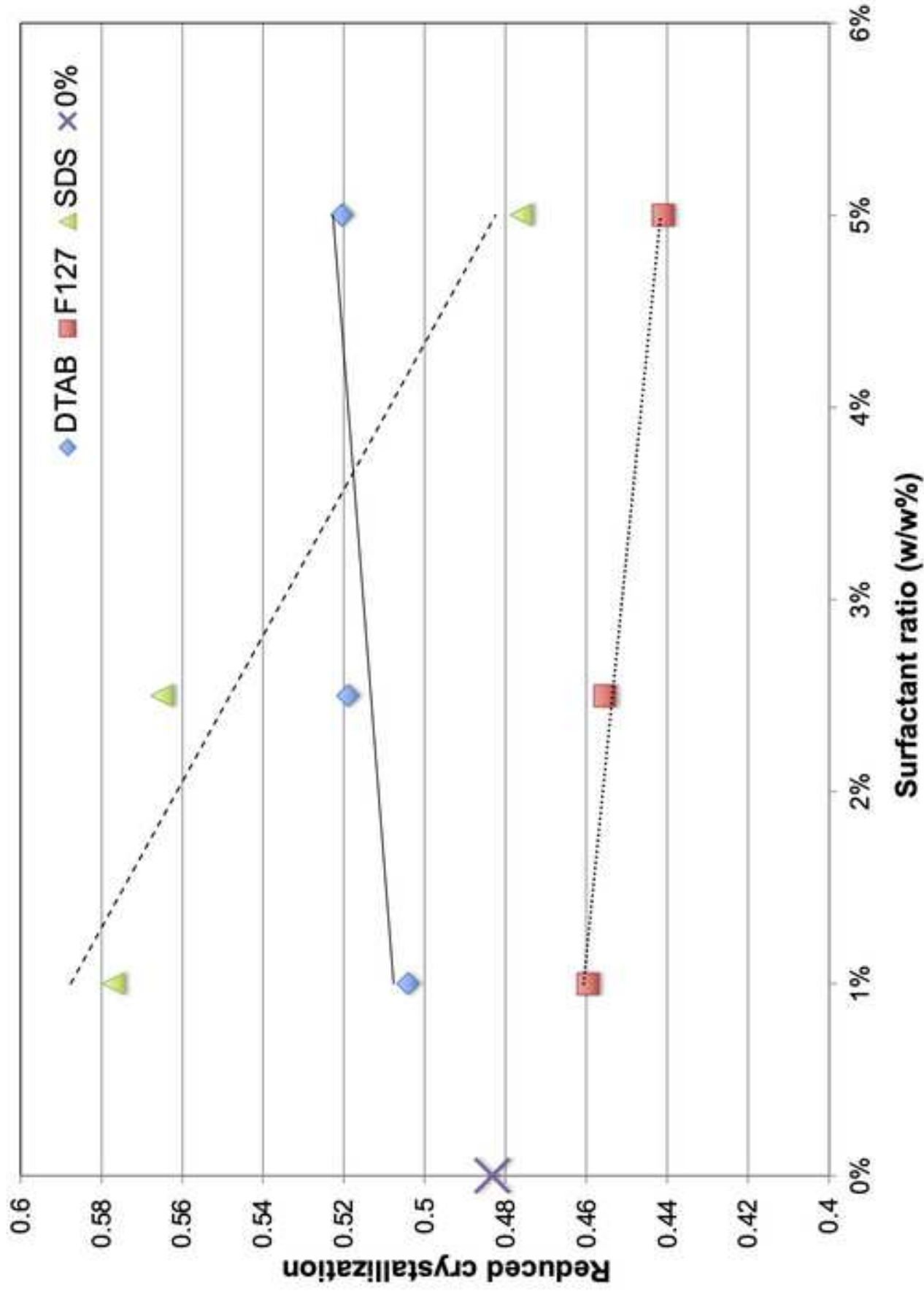
Figure 3

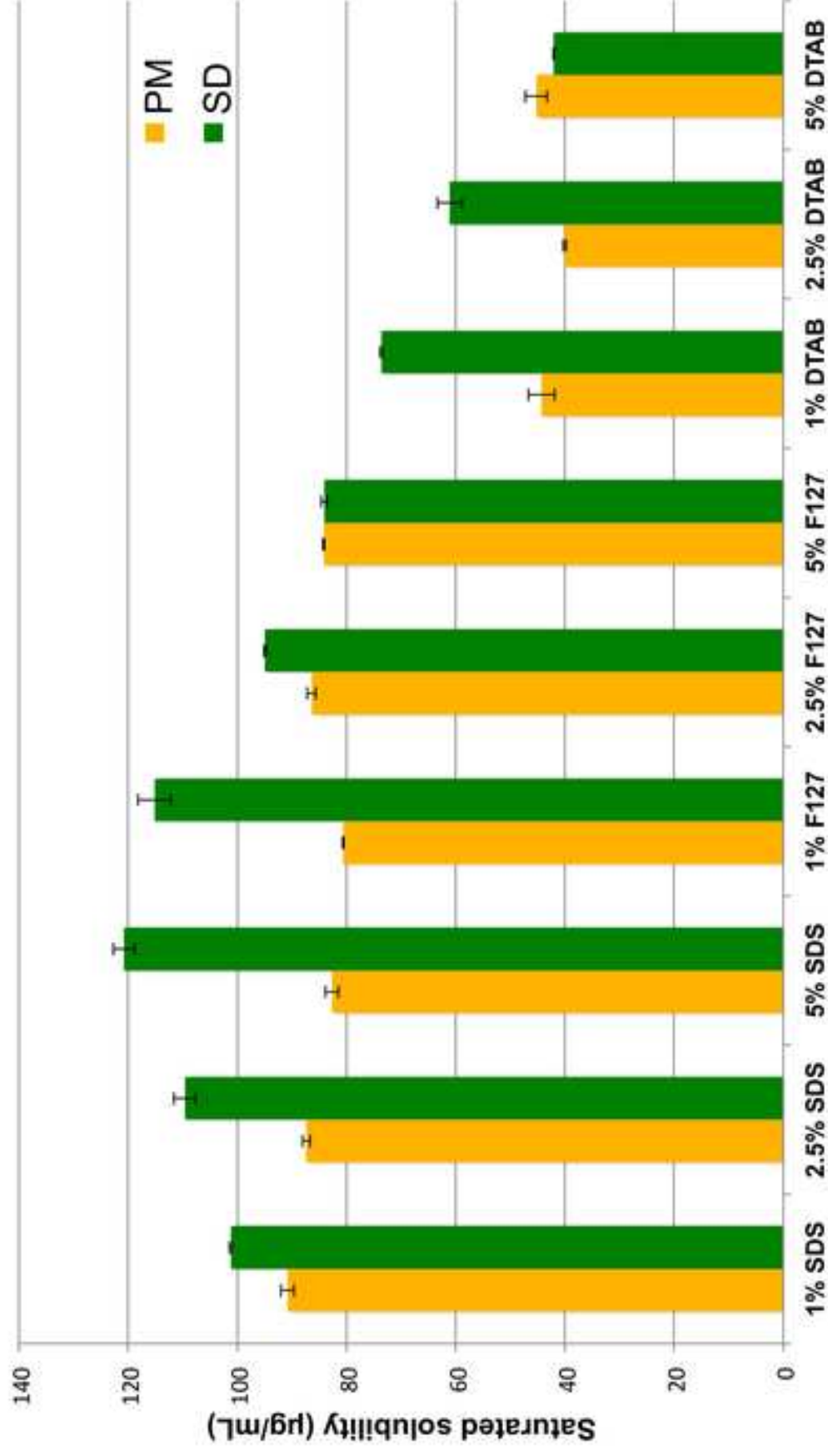
[Click here to access/download;Figure;Figure 3_.jpg](#)



[Click here to access/download;Figure 4_.jpg](#)







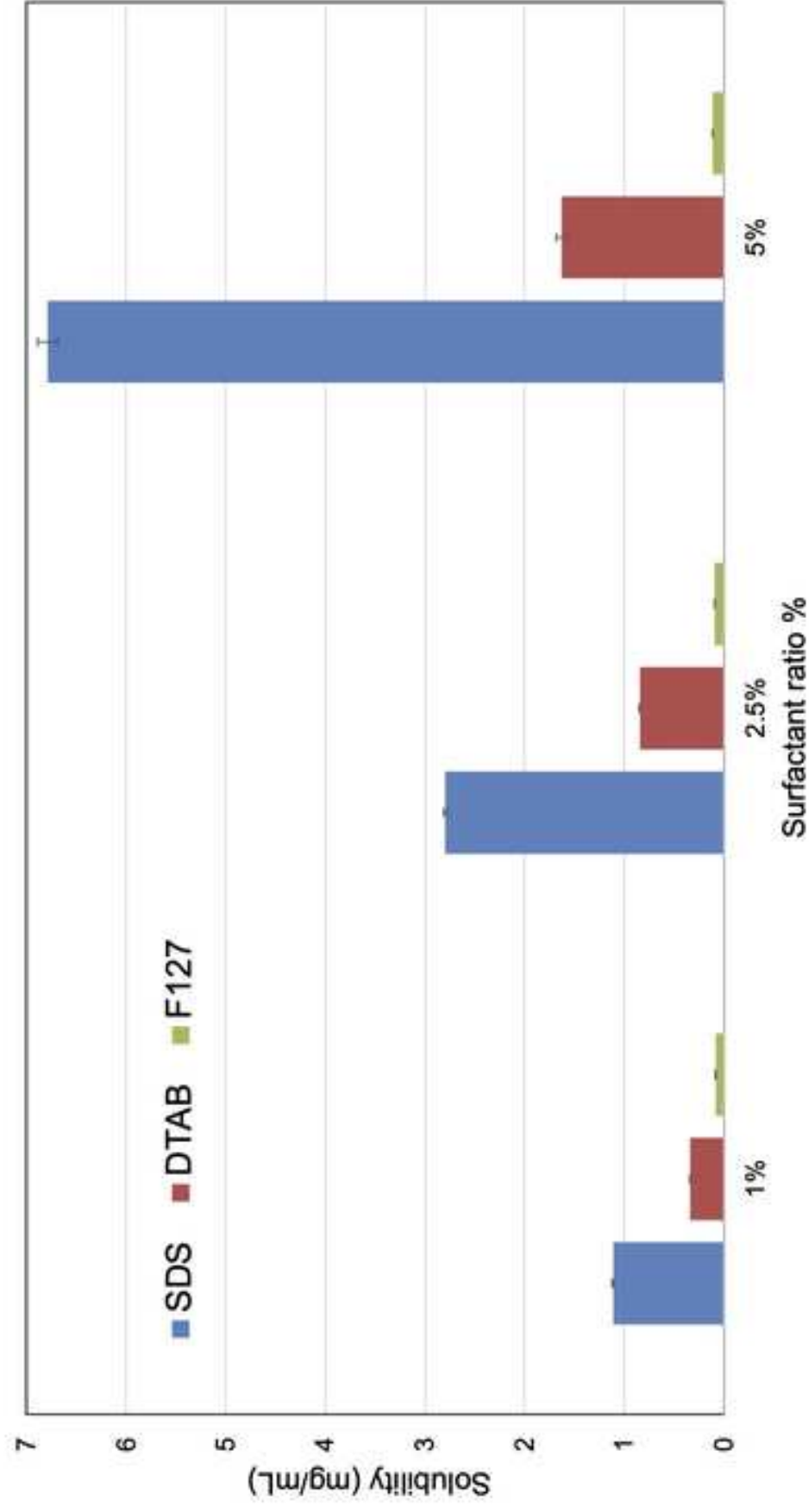


Figure 8

[Click here to access/download;Figure;Figure 8_.jpg](#)

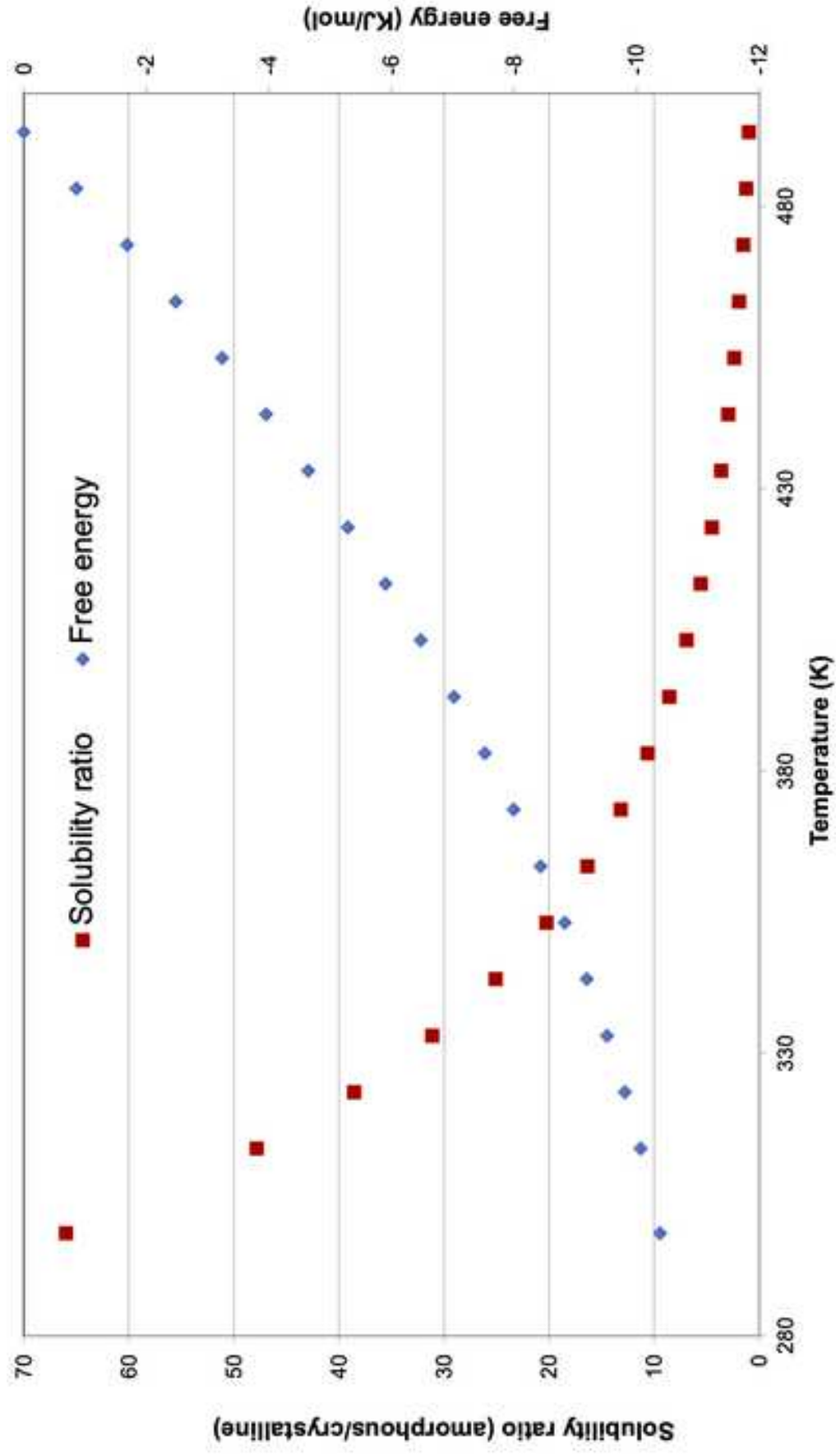
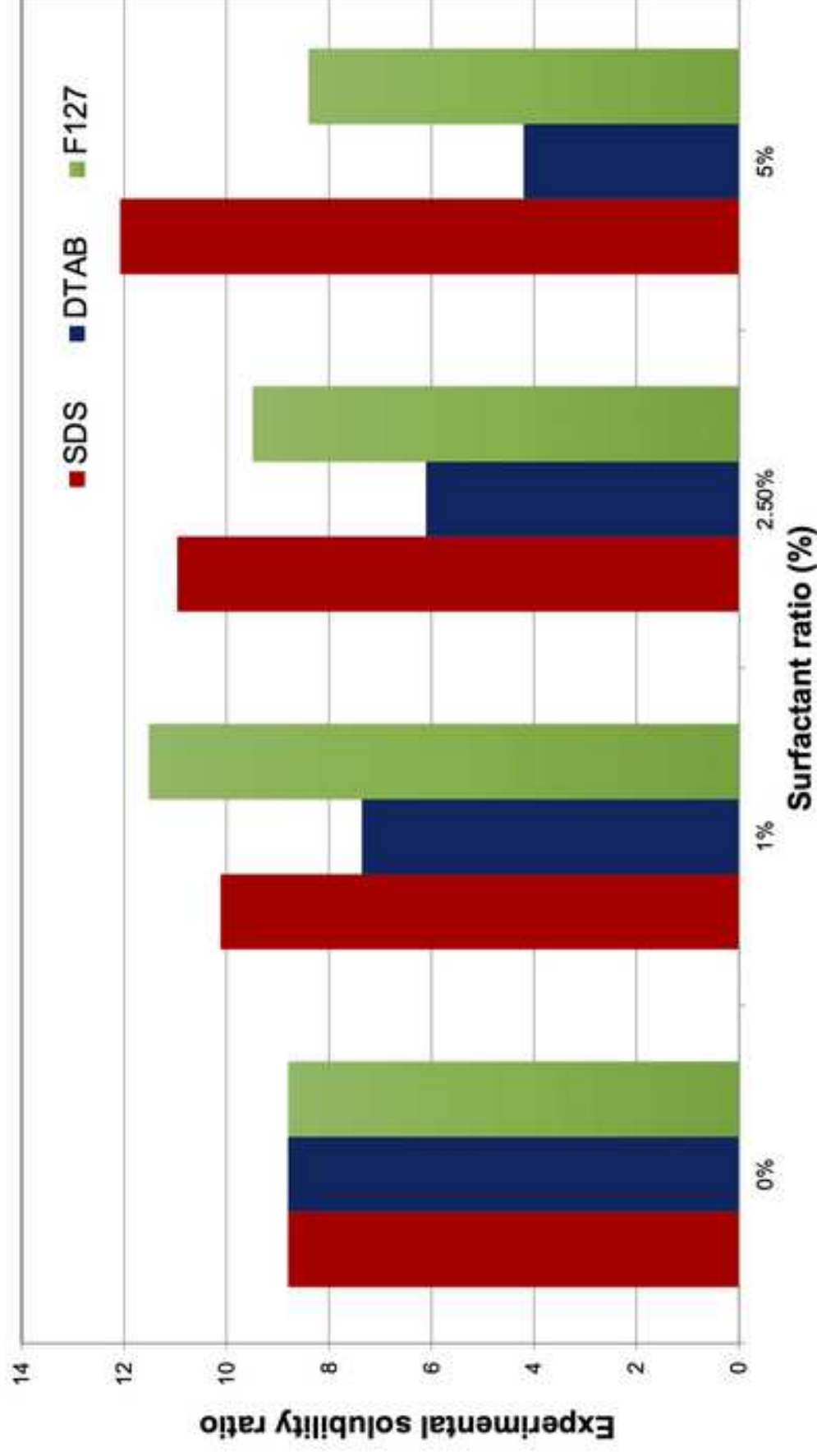
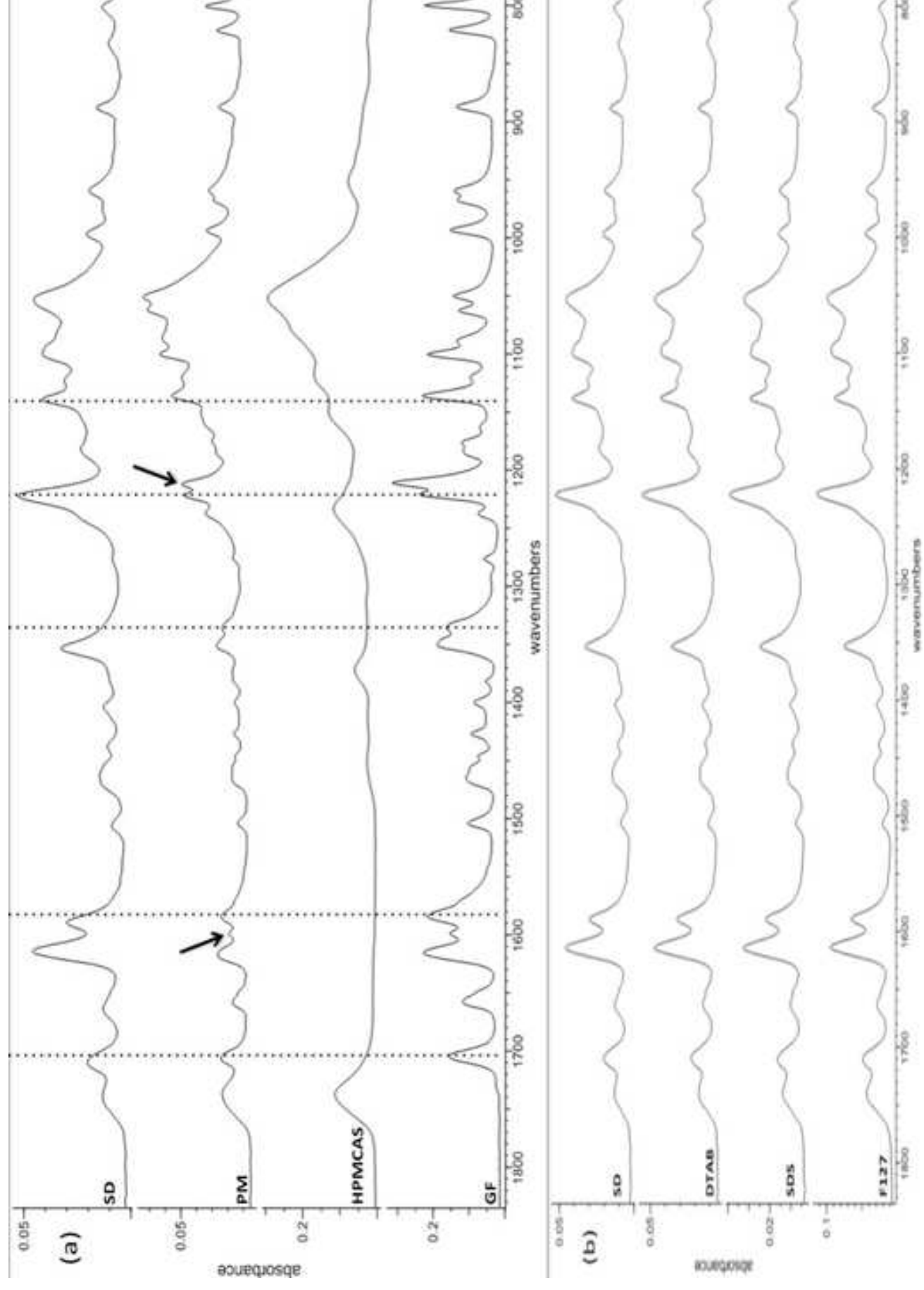


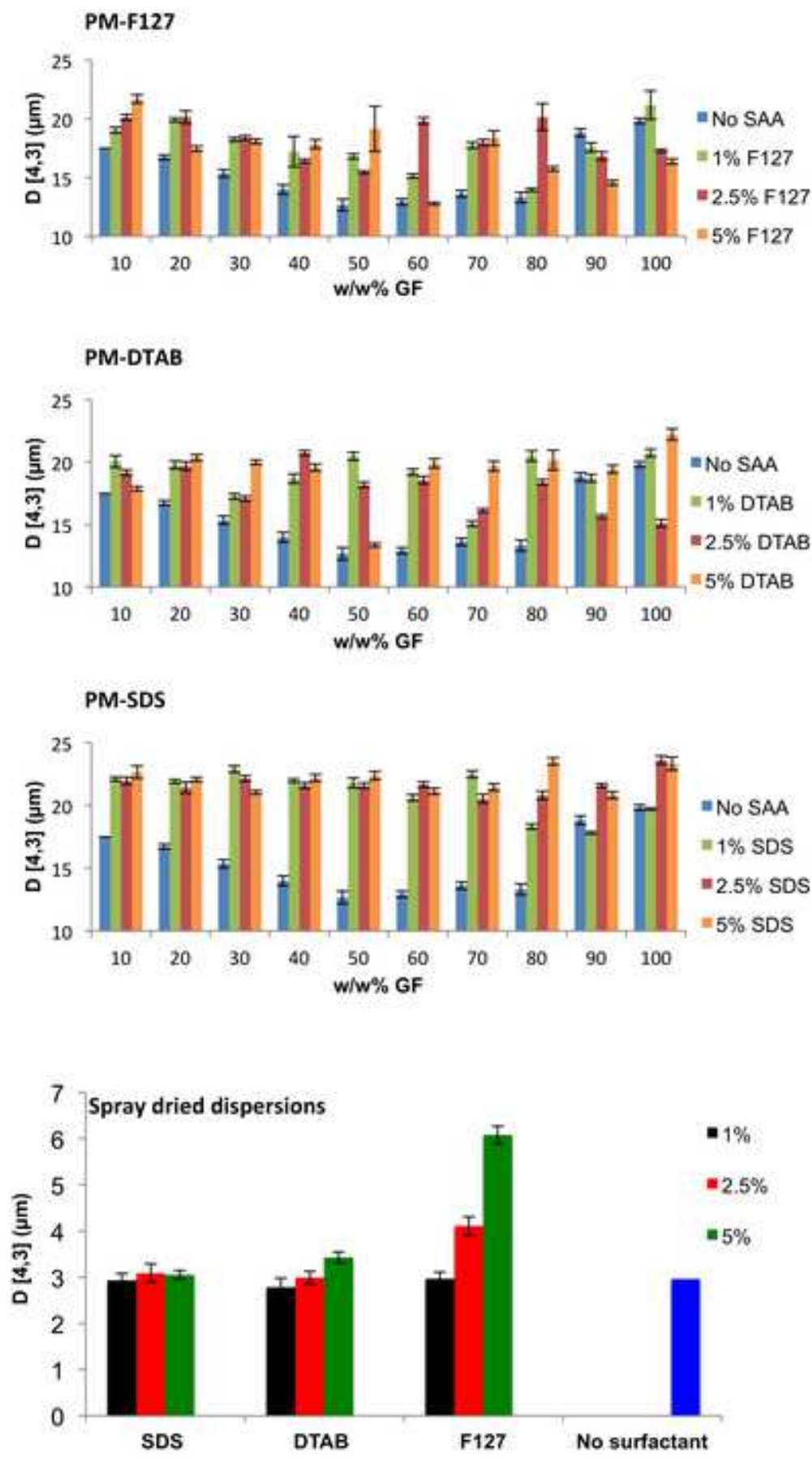
Figure 9

[Click here to access/download;Figure;Figure 9_.jpg](#)









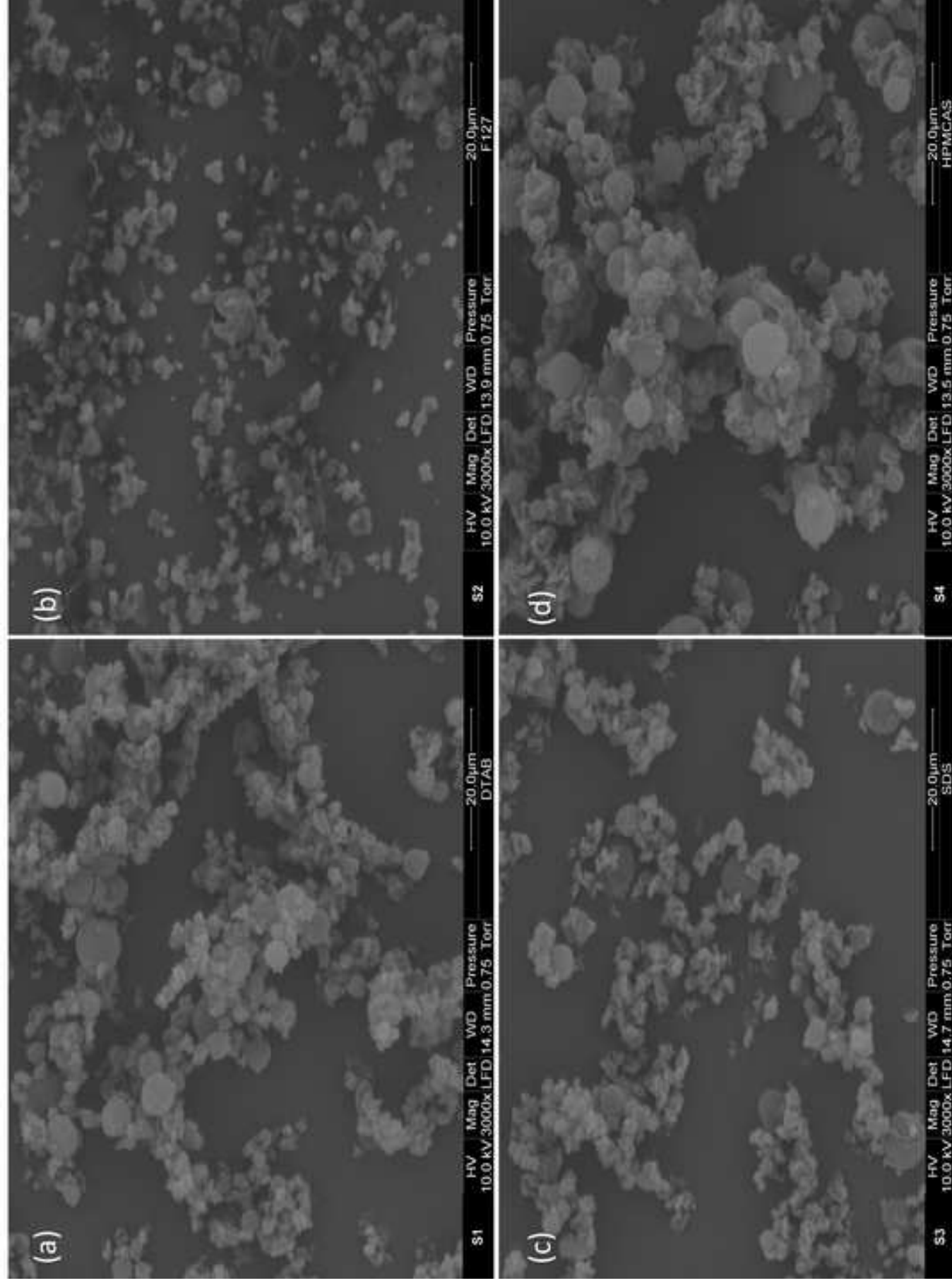


Table 1: Mass ratios (expressed as w/w%) of GF, HPMCAS and surfactant (SDS, DTAB or F127) that were used to prepare the physical mixtures.

Surfactant	GF	HPMCAS	Surfactant	GF	HPMCAS	Surfactant	GF	HPMCAS	Surfactant	GF	HPMCAS
0	10	90	1	9.5	89.5	2.5	8.75	88.75	5	7.5	87.5
0	20	80	1	19.5	79.5	2.5	18.75	78.75	5	17.5	77.5
0	30	70	1	29.5	69.5	2.5	28.75	68.75	5	27.5	67.5
0	40	60	1	39.5	59.5	2.5	38.75	58.75	5	37.5	57.5
0	50	50	1	49.5	49.5	2.5	48.75	48.75	5	47.5	47.5
0	60	40	1	59.5	39.5	2.5	58.75	38.75	5	57.5	37.5
0	70	30	1	69.5	29.5	2.5	68.75	28.75	5	67.5	27.5
0	80	20	1	79.5	19.5	2.5	78.75	18.75	5	77.5	17.5
0	90	10	1	89.5	9.5	2.5	88.75	8.75	5	87.5	7.5

Table 2: Residual solvent content measured using thermogravimetric analysis (TGA) of spray dried amorphous solid dispersions prepared using GF:HPMCAS (50%:50%) with 5% surfactant.

Surfactant added	Physical Mixture	Spray Dried Solid Dispersion
No added surfactant	1.1%	1.4 %
5% SDS	1%	0.9%
5% PF-127	0.9%	0.9%
5% DTAB	0.8%	1%